Transport in Porous Media (2007) 66:259–286
DOI 10.1007/s11242-006-0017-9

Pore-scale Simulation of Water Alternate Gas Injection

V. SANDER SUICMEZ[1,⋆], MOHAMMAD PIRI[2] and MARTIN J. BLUNT[1]
[1]*Department of Earth Science and Engineering, Imperial College London, London SW7 2AZ, UK*
[2]*Department of Chemical and Petroleum Engineering, University of Wyoming, Laramie, Wyoming 82071, USA*

(Received: 27 October 2005; accepted in final form: 31 January 2006)

Abstract. We use a three-dimensional mixed-wet random network model representing Berea sandstone to compute displacement paths and relative permeabilities for water alternating gas (WAG) flooding. First we reproduce cycles of water and gas injection observed in previously published experimental studies. We predict the measured oil, water and gas relative permeabilities accurately. We discuss the hysteresis trends in the water and gas relative permeabilities and compare the behavior of water-wet and oil-wet media. We interpret the results in terms of pore-scale displacements. In water-wet media the water relative permeability is lower during water injection in the presence of gas due to an increase in oil/water capillary pressure that causes a decrease in wetting layer conductance. The gas relative permeability is higher for displacement cycles after first gas injection at high gas saturation due to cooperative pore filling, but lower at low saturation due to trapping. In oil-wet media, the water relative permeability remains low until water-filled elements span the system at which point the relative permeability increases rapidly. The gas relative permeability is lower in the presence of water than oil because it is no longer the most non-wetting phase.

Key words: network modeling, three-phase flow, wettability, relative permeability, multiple displacements, pore occupancy.

1. Introduction

Even though petroleum and natural gas resources are finite, they remain among the most important sources of energy in the world. With the decline of hydrocarbon reserves, improved recovery of these resources to boost production is becoming increasingly important. Most improved oil recovery projects involve the flow of three phases, where a gas, which could be air, natural gas, CO_2 or steam, is injected into a reservoir containing oil and

⋆Author for correspondence: e-mail:vss@imperial.ac.uk

water (Lake, 1989). In particular, the use of CO_2 injection into mature oil fields is likely to become increasingly common not only to enhance oil recovery but for storage of CO_2 emitted from power stations and other large point sources. To predict recovery and to design an improved oil recovery scheme, one needs to input the constitutive relationships between macroscopic properties such as relative permeability, capillary pressure and phase saturations into the simulation model.

Experimental measurements of three-phase flow are extremely difficult to perform and the results are frequently not reliable at low saturation (Oak, 1991). In addition to the measurement of saturations, pressure drops, and fluxes in three flowing phases, there are an infinite number of different displacement paths. Thus it is impractical to measure relative permeability for all possible three-phase displacements that may occur in reservoir. As a result, the universal practice in reservoir simulation studies is to estimate three-phase relative permeabilities using empirical correlations, which usually have very little or no physical basis (Stone, 1970, 1973; Baker, 1988; Blunt, 2000).

Water alternating gas (WAG) injection is one of the many improved oil recovery methods that involve three-phase fluid flow. It was originally proposed as a method to improve the sweep efficiency of gas by using water to control the mobility ratio and to stabilize the front (Caudle and Dyes, 1958; Christensen *et al.*, 1998). Although WAG flooding has been successfully applied to more than 60 oilfields worldwide, there is still an incomplete understanding of the pore-scale physics of the process and how it leads to improved oil recovery, especially in systems with non-uniform wettability. The major problems in the evaluation of WAG behavior are uncertainties regarding the prediction of the wettability and spreading conditions as well as the relative permeabilities of the phases for different injection cycles.

Since gas is generally the most mobile phase during WAG flooding, the gas relative permeability controls the efficiency of the process. Gas is the most non-wetting phase in water-wet systems. As a consequence gas invades the largest pores and throats. However, during wetting phase injection (water or oil flooding), gas is displaced from the smaller pores that it occupies. Although the saturation of the gas phase may not be affected significantly, this causes disconnection of continuous gas clusters, reducing the gas phase relative permeability. It has been observed that continued cycles of gas/water injection lead to progressively lower gas relative permeability and additional oil recovery in both micromodel and core experiments (Egermann *et al.*, 2000; Sohrabi *et al.*, 2000; Element *et al.*, 2003; Feng *et al.*, 2004 van Dijke *et al.*, 2004). However, most reservoirs are mixed- or oil-wet where gas is not necessarily the most non-wetting phase. Gas can be the intermediate wet phase in a strongly oil-wet medium (DiCarlo *et al.*, 2000a, b) meaning that the displacement mechanisms and pore occupancies are expected to be different. However, the literature data on WAG flooding in non-water-wet systems is very limited. Furthermore, most of the widely used empirical correlations are developed with an assumption that the rock is strongly water-wet (Blunt, 2000). This is why empirical equations fail to predict three-phase relative permeabilities accurately for non-water-wet conditions (Element *et al.*, 2003).

Skauge and Larsen (1994) proposed a relative permeability hysteresis model for WAG processes and validated it with experimental data. They conducted experiments on Berea sandstone cores with different wettability conditions. It was observed that hysteresis was more pronounced for the non-wetting phase while the wetting phase relative permeability was found to be a function of its own saturation. The trapped gas saturation was fitted to a Land-type of equation (Land, 1968). Reservoir simulations based on the new hysteresis model showed a reasonable agreement with the measured effluent production and differential pressure.

In recent years, our fundamental physical understanding of three-phase flow at the pore level has advanced significantly (Øren *et al.*, 1992; Blunt, 2000). Several authors have developed network models to simulate two- and three-phase fluid flow at the pore scale (Fenwick and Blunt, 1998a, b; Mani and Mohanty, 1998; Øren *et al.*, 1998; van Dijke and Sorbie, 2002; Valvatne and Blunt, 2004; van Dijke *et al.*, 2004; Piri and Blunt, 2005a). In the last decade, promising progress has been made in predicting three-phase relative permeabilities using pore network models (Fenwick and Blunt, 1998a, b; Svirsky *et al.*, 2004; Piri and Blunt, 2005b).

One unique feature of three-phase flow is that displacement may involve one or more disconnected clusters, such as when water displaces a trapped cluster of gas that then displaces oil. Double displacement, involving a single trapped cluster, has been observed in micromodel experiments (Øren *et al.*, 1992; Keller *et al.*, 1997) and has been coded into network models (Øren *et al.*, 1994; Fenwick and Blunt, 1998b; Mani and Mohanty, 1998; Piri and Blunt, 2005a). van Dijke *et al.* (2004) demonstrated using a combination of pore-scale simulation and micromodel experiments (Sohrabi *et al.*, 2000) that for media with low phase connectivity, multiple displacements, involving trapped clusters of more than one phase, need to be considered, since repeated water and gas cycles increase the number of trapped clusters significantly.

van Dijke and Sorbie (2003) investigated the occurrence and impact of multiple displacements during WAG injection. They concluded that multiple displacement is an important mechanism for the trapping and remobilization of gas and oil, especially in media with a low coordination number and poor connectivity of wetting and spreading layers. Svirsky *et al.* (2004) extended the work of van Dijke and Sorbie (2003) by predicting three-phase relative permeability using a network model anchored to two-phase data. They first matched experimental two-phase data (Oak, 1990) using several free parameters such as volume and conductance exponents, pore-throat size distribution, coordination number and contact angles. Then they predicted the three-phase relative permeabilities, which were in good agreement with the experimental data. The authors used same parameters for conducting generic WAG simulations with different spreading and wettability conditions. It was shown that there is a significant decrease in gas relative permeability with subsequent injection cycles for water-wet and mixed-wet systems.

Piri and Blunt (2005a, b) presented a three-dimensional mixed-wet network model in order to simulate two- and three-phase fluid flow. A random network, generated by using process-based techniques (Øren and Bakke, 2002), was used to represent the pore space in Berea sandstone. The model simulated any sequence of oil, water and gas injection. Threshold capillary pressures for all possible displacements were computed for 30 different phase configurations. Two- and three-phase relative permeabilities were successfully predicted and compared with the steady state experiments conducted by Oak (1990). They also studied secondary and tertiary gas injection into media of different wettability and initial oil saturation. The only multiple displacement process considered by Piri and Blunt (2005a) was double drainage where gas displaces trapped oil that displaces water. However, in WAG flooding, double and multiple displacement processes involving trapped gas will also be important.

In this paper, we extend the work of Piri and Blunt (2005a, b) by adding two new double displacement processes that involve trapped gas. We briefly describe the model and introduce the new displacement mechanisms. We then compare our predictions with experimental data as well as conducting sensitivity runs with varying wettability conditions. The advantage of this model over the work of van Dijke *et al.* (2004) and Svirsky *et al.* (2004) is that the network explicitly represents a real rock and hence we are able to make first-principles computations with no adjustable parameters. The disadvantage is that we consider only double displacement – displacements involving trapped clusters of more than one phase are ignored. In the Berea network 99.7% of the elements have angular (square or triangular) cross-sections where water is connected in corners. As a consequence only gas and oil are trapped. We study a spreading system, which means that the oil is normally connected in the presence of gas. As a consequence, as we show later, double displacements, although important, are rare in comparison with direct displacement of one connected phase by another and we suggest that in the cases we study higher order displacements are uncommon.

2. Network Modeling

The fluids used in this work are assumed to be Newtonian, incompressible, and immiscible. Displacement at the pore scale is assumed to be quasi-static and capillary dominated. A displacement is defined as a change in the configuration of an element (pore or throat) in order to satisfy the capillary equilibrium conditions. This can either be a displacement of a phase by another in the center of an element or layer collapse/formation in a single corner. Each displacement has a threshold capillary pressure associated with it. The properties of the Berea sandstone network, the analytical calculations of the threshold pressures as well as the possible fluid configurations have already been discussed in the literature (Øren *et al.*, 1998; Hui and Blunt, 2000; Piri and Blunt, 2005a). The Berea network contains 12,000 pores and 26,000 throats. In the network, each pore and throat is assumed to have an irregular triangular, square or circular cross-section. Full details of the model are provided in Piri and Blunt (2005a).

2.1. SINGLE DISPLACEMENTS

For every single displacement, there is a displacing phase and a displaced phase. Each displacement is either drainage or imbibition. If a wetting phase is displaced by a non-wetting phase, the displacement is called drainage; if non-wetting phase is displaced by the wetting phase then the displacement is imbibition. A displacement occurs at threshold pressure of the displacing phase. However, there might be more than one available displacement. In that case, the displacement with the lowest threshold pressure will be performed first.

Displacements may be categorized into four sub-groups: piston-like, pore-body filling, snap-off and layer collapse and formation. Piston-like refers to the displacement of one phase by another through the center of a throat. Due to contact angle hysteresis, the threshold capillary pressure for piston-like displacement can be different for drainage and imbibition events. Pore-body filling refers to the displacement of one phase in the center of a pore by the displacing phase located in the centers of adjoining throats. For a drainage event, the threshold capillary pressure is given by similar expressions for piston-like advance. However the imbibition threshold capillary pressure for the displacement depends on the number of neighboring throats that hold the invading phase and are able to contribute to the displacement (Lenormand *et al.*, 1983). Snap-off corresponds to an imbibition event where the non-wetting phase located at the center of the element is displaced by the wetting phase, which is located either in the corners or in the layers of the element. If the center of a neighboring element holds the invading phase, piston-like displacements would be favored and snap-off does not occur.

The model developed by Piri and Blunt (2005a) considers the layer collapse and formation events as separate displacements. Depending on the contact angles, capillary pressures, and corner half angles, layers may be formed through displacements by the fluids residing in the centers or the layers of the neighboring elements. Once a layer forms, it is possible to collapse this layer with an increase in the pressure of the fluids residing on either side of the layer (corner or center). Sometimes the same phase (water) may be residing both in the corner and center of the element next to either a gas or an oil layer, in which case both the center and the corner contribute to the layer collapse event if the pressure of the water phase increases.

2.2. MULTIPLE DISPLACEMENTS

In two-phase static network models, a fluid phase is able to move and contribute to displacement events only if it is connected to the inlet or outlet. In three-phase flow, however, the displacement of trapped clusters is vital for predicting recovery mechanisms: for instance oil that is trapped during waterflooding becomes reconnected by gas through the pore-scale migration and coalescence of oil clusters. Our model only considers double displacement. There are six possible double displacements (Table I) out of which only double drainage (gas displacing oil and displaced oil displacing water) was included in the model developed by Piri and Blunt (2005a), since the authors were mainly interested in tertiary gas injection. However, to simulate WAG injection appropriately, where both oil and gas are trapped, we extended this model by including two other double displacement processes: double imbibition (water displacing trapped oil that

Table I. Possible double displacement processes for a water-wet medium (Fenwick and Blunt, 1998b). Depending on wettability, the name of the displacement may change, but the sequence of phase displacement remains same

Name	Displacement sequence
Double Drainage	Gas displaces oil and oil displaces water
Drainage–Imbibition	Gas displaces water and water displaces oil
Imbibition–Drainage	Water displaces gas and gas displaces oil
Double Imbibition	Water displaces oil and oil displaces gas
Imbibition–Drainage	Oil displaces gas and gas displaces water
Drainage–Imbibition	Oil displaces water and water displaces gas

displaces gas) and imbibition-drainage (water displaces trapped gas that displaces oil). Since we do not consider oil injection and water is almost always continuous, the three other double displacement mechanisms are ignored.

When a double displacement is carried out, the displacement can be considered as two single displacements. The first one is a continuous phase displacing a trapped phase, and the second one is displaced trapped phase displacing another continuous phase. To perform the displacement, we first increase the trapped phase pressure to the threshold pressure of the second single displacement (trapped phase displacing the continuous phase). Then, by adding this difference to the threshold pressure of the first single displacement (continuous phase displacing the trapped phase), we can calculate the threshold pressure for the double displacement event. It is given as:

$$P_{DD}^{\text{threshold}} = P_{\text{first}}^{\text{threshold}} + P_{\text{second}}^{\text{threshold}} - P_{\text{trapped}}, \tag{1}$$

where P is the pressure, DD stands for double displacement, *first* is the displacement of trapped phase by a continuous phase, and *second* is the displacement of the continuous phase by the displaced trapped phase.

3. Results and Discussion

We will use the network model to predict three experimental datasets: Oak (1990), Egermann *et al.* (2000) and Element *et al.* (2003) before using the model to predict trends in behavior with wettability.

3.1. OAK DATA

Piri and Blunt (2005b) successfully predicted the relative permeabilities of tertiary gas injection experiments conducted by Oak (1990) and then predicted the behavior in an oil-wet system. They showed that double drainage allows oil to become reconnected when gas is injected, discussed the differences in oil relative permeability as a function of water and gas saturations and demonstrated that the oil relative permeability for secondary gas injection is proportional to the square of the oil saturation. We extend this work by simulating both simultaneous and cyclic gas/water injection experiments conducted by Oak (1990). Current empirical relative permeability models are unable to predict this data accurately (Spiteri and Juanes, 2004). Although the wettability and the spreading conditions of the medium are not clearly presented in the experimental work, we assume a water-wet and spreading oil system (Table II). The same properties have been used to predict successfully Oak's two-phase data and three-phase gas injection relative permeability (Valvatne and Blunt, 2004; Piri and Blunt,

Table II. The interfacial tension and contact angle values used in our model to predict Oak's experiments (1990)

σ_{gw}(mN/m)	67
σ_{go}(mN/m)	19
σ_{ow}(mN/m)	48
θ^{r}_{gw}(degrees)	36.6–57.3
θ^{r}_{go}(degrees)	10–50
θ^{r}_{ow}(degrees)	43–60
θ^{a}_{gw}(degrees)	55.2–77.2
θ^{a}_{go}(degrees)	30–70
θ^{a}_{ow}(degrees)	63–80

2005b). The success of these studies suggests that the fluid properties are representative of the experiments and that the Berea network is an adequate description of the Berea cores studied by Oak.

The network model considers a sequence of water and gas displacements that track the experimental displacement path (Piri and Blunt, 2005a). Tracked and measured saturation paths as well as the comparison of predicted and measured three-phase relative permeabilities are shown in Figures 1–8. The results show that the relative permeability predictions are good for both simultaneous (Figures 1–4) and cyclic (Figures 5–8) gas/water injection. During simultaneous gas/water injection, although we obtain excellent predictions for the water relative permeability, we underestimate oil relative permeability at low oil saturation (Figure 3). In this region, oil resides principally in layers in the pore space sandwiched between water in the corners and oil in the center. The oil relative permeability is controlled by layer drainage. It is possible that we underestimate the conductance or stability of these layers. This result though is different from that obtained by Piri and Blunt (2005b) for gas injection, where the oil relative permeability was overestimated at low saturation. The conclusion here is that the quantitative behavior of the oil drainage regime requires further study. In particular, the expressions we use for oil layer stability are not based on strict thermodynamic criteria (van Dijke *et al.*, 2004). We overestimate the saturation at which gas breakthrough occurs (Figure 4). This is a finite size effect, since our network represents a considerably smaller system than the cores studied experimentally (Wilkinson and Willemson, 1983; Blunt *et al.*, 1992).

Figure 5 shows the experimental displacement path for a case where there are cycles of water and gas injection. Gas injection is performed into water and residual oil and then water is injected again until both gas and oil are trapped. The match to the saturation path using network modeling

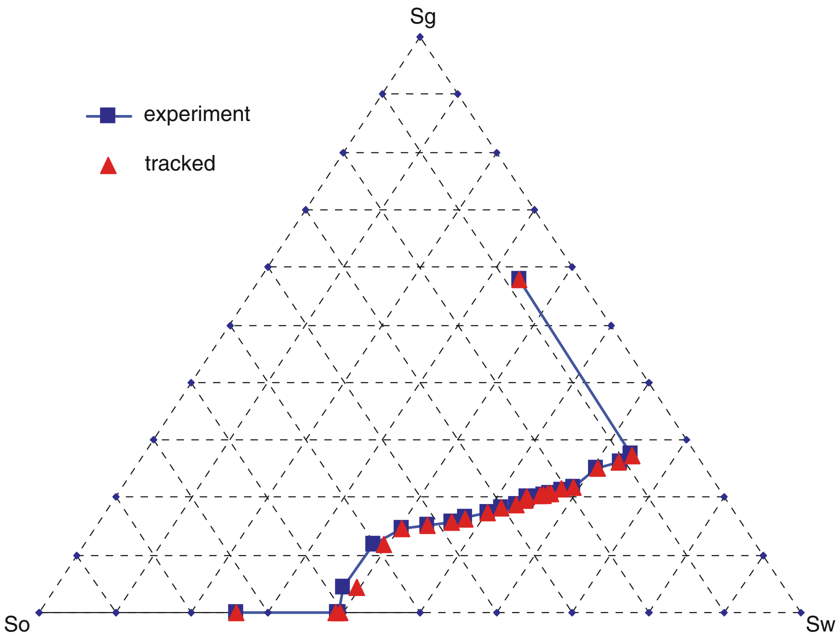

Figure 1. Comparison of measured and tracked saturation paths for simultaneous water and gas injection. Experiment 14 – Sample 13 of Oak experiments (Oak, 1990).

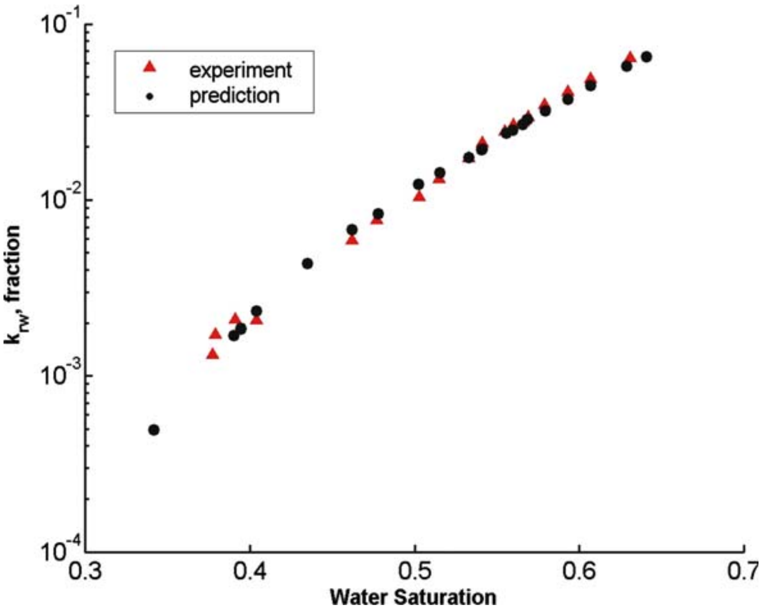

Figure 2. Comparison of measured and predicted water relative permeabilities for the saturation path shown in Figure 1.

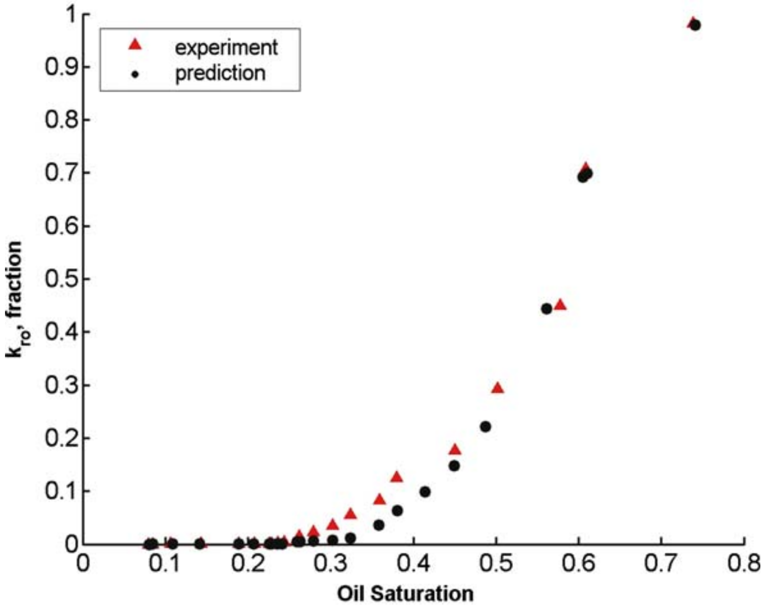

Figure 3. Comparison of measured and predicted oil relative permeabilities for the saturation path shown in Figure 1.

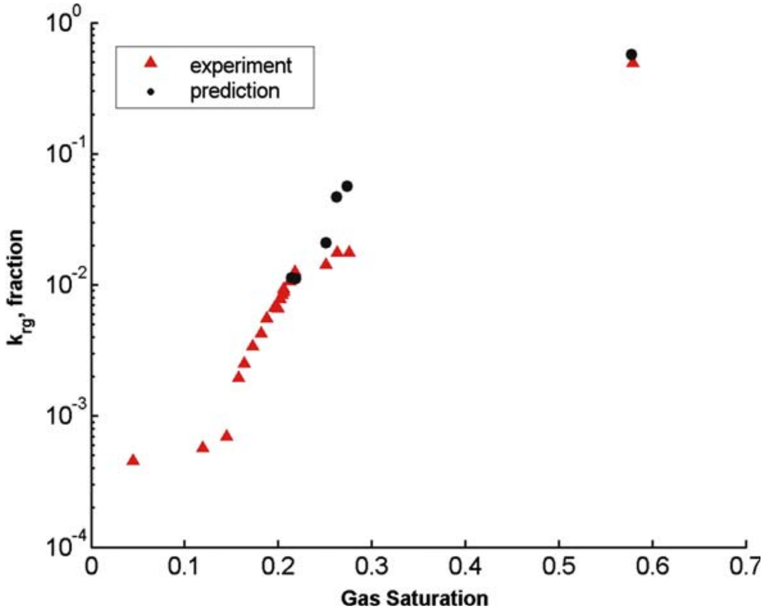

Figure 4. Comparison of measured and predicted gas relative permeabilities for the saturation path shown in Figure 1.

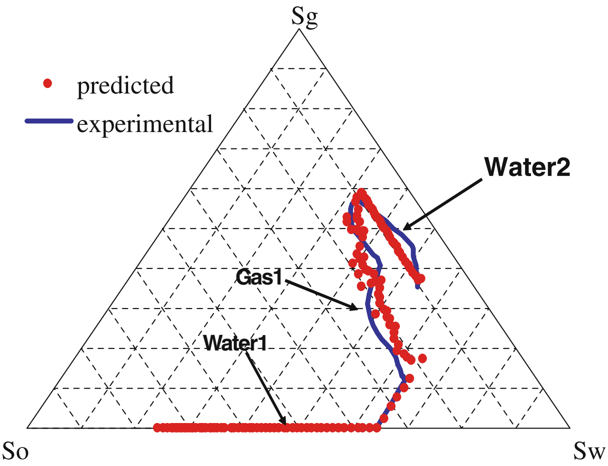

Figure 5. Comparison of measured and tracked saturation paths for cyclic gas and water injection. Experiment 4 – Sample 6 of Oak experiments (Oak, 1990).

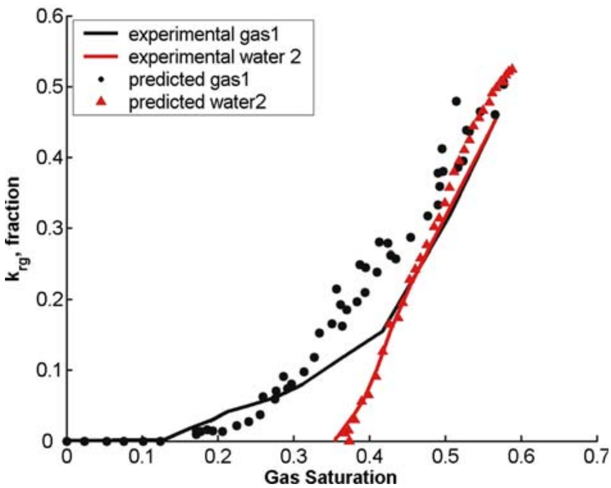

Figure 6. Comparison of measured and predicted gas relative permeabilities for the saturation path shown in Figure 5.

is good as are the predictions of relative permeability (Figures 6–8). Gas is the most non-wetting phase and a significant decrease in the gas relative permeability is observed during secondary water injection (Figure 6). The reason for this is that water traps gas, principally through snap-off, which is predicted accurately by the pore-scale model confirming other experimental and numerical studies (Skauge and Larsen, 1994; Svirsky *et al*., 2004). As can be seen from Table III, there are a significant number of water to gas snap-off displacements during secondary water injection, although the most common mechanism is piston-like advance.

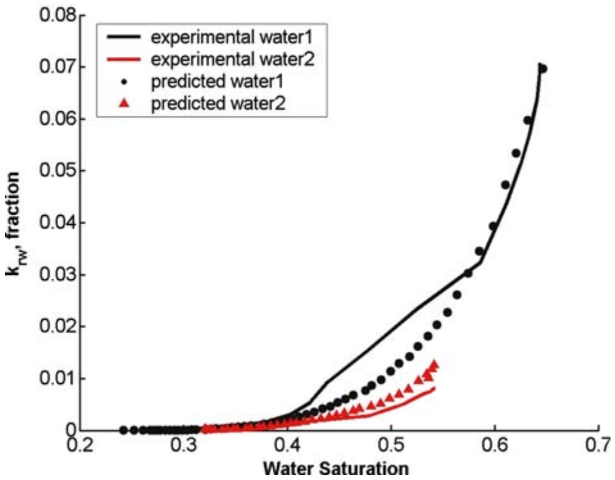

Figure 7. Comparison of measured and predicted water relative permeabilities for the saturation path shown in Figure 5.

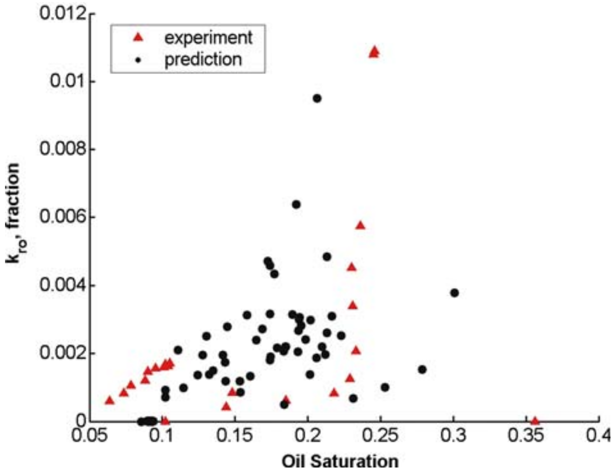

Figure 8. Comparison of measured and predicted oil relative permeabilities for gas 1 and water 2 cycles shown in Figure 5.

Table III. Statistics for water to gas displacements during the secondary water injection process for the saturation path shown in Figure 5

	Piston-like	Snap-Off
Number	13,041	963
Percentage (%)	92.6	7.4

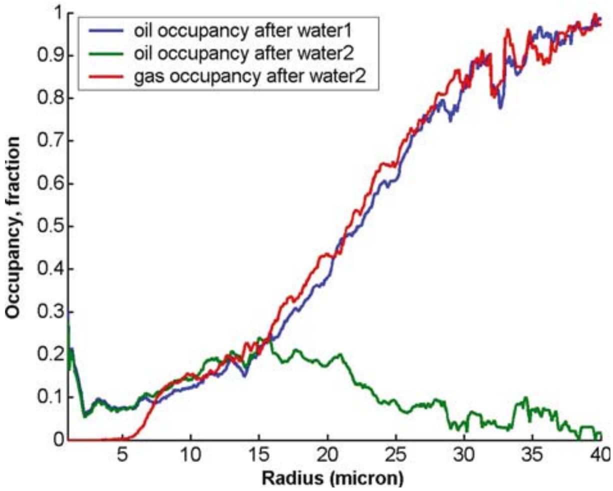

Figure 9. Pore occupancies for the first and second water injection cycles for the saturation path shown in Figure 5.

An unexpected observation is the noticeable water relative permeability hysteresis (Figure 7) evident in both the experiments and the predictions. Since water is the most wetting phase, it is not trapped and resides in the smallest elements of the pore space. The traditional thinking is that as a consequence the water relative permeability is a function of its own saturation only and does not display any hysteresis (Stone, 1970). However, we find that the water relative permeability is lower for the second water injection (water injected into a high gas saturation) than for the first (water displacing oil with no gas present). Figure 9 shows the gas and oil pore occupancies after the first and second water injection processes. Once we introduce gas into the system, oil no longer occupies the biggest pore and throat elements. Instead gas, which is the most non-wetting phase in a water-wet system, moves oil into smaller pores and throats by single and double displacement. Most of this oil is trapped. In the network model, if trapped clusters become reconnected, the continuous phase pressure is increased to that of the trapped phase (van Dijke and Sorbie, 2002; Piri and Blunt, 2005a). This approach allows the oil/water capillary pressure to increase during gas injection through the reconnection of previously trapped oil, as evident in Figure 10 and observed in micromodel experiments (van Dijke *et al.,* 2004). When water re-injection commences, the oil/water capillary pressure increases sharply. This counter-intuitive result – in two-phase flow the capillary pressure decreases when imbibition starts – is due to the reconnection of some trapped oil in the smallest pores and throats through single and multiple displacement. The magnitude of the capillary pressure is consistent with the reconnection of oil that was

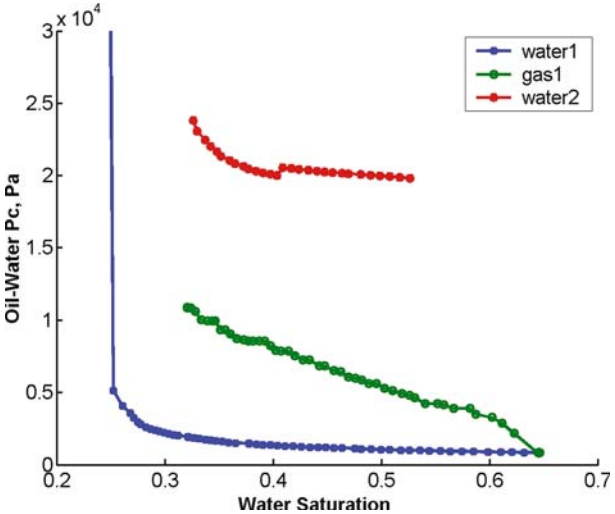

Figure 10. Oil–water capillary pressure for the first water, first gas, and second water injection cycles for the saturation path shown in Figure 5.

displaced into elements of radius 2–3μm by double drainage during gas injection. This increase in capillary pressure means that oil pushes water further into the corners of the pore space. The water relative permeability is controlled by the conductance of water in the corners of elements whose centers are oil or gas filled. As water is pushed into the corners, this conductance decreases sharply, causing the observed decrease in water relative permeability. While the predictions of relative permeability agree with the experimental measurements, it is not certain that our assumption of assigning the trapped phase pressure to the continuous phase on reconnection correctly represents the pore-scale processes occurring in the experiments.

After the first water injection, oil is disconnected and has a zero relative permeability. During gas injection the oil is reconnected due to double drainage when gas pushes oil into smaller elements. Since volume is conserved, the oil now occupies more pores and throats and quickly fills a sufficient fraction of the network to become connected. In addition, due to spreading layers, oil remains connected in elements that contain gas. The oil relative permeability is then finite but decreases as further gas invasion displaces oil. At the end of gas invasion, the oil relative permeability is close to zero, as connected oil resides in only a few smaller elements and in oil layers. There are also trapped clusters of oil in elements where no layers are present. As shown in Figure 8, when water is re-injected, the oil relative permeability again increases slightly, as double imbibition allows trapped oil clusters to reconnect. Because the oil is becoming connected and disconnected through repeated flooding cycles, both the experimental and numerical data are noisy, but we predict the experimental trend in behavior.

Table IV. Displacement statistics for the first gas injection and secondary water injection cycles for the saturation path shown in Figure 5

Type/Cycle	1st gas cycle (%)	2nd water cycle (%)
Gas–oil-water	14.4	–
Gas–oil	27.4	–
Gas–water	58.2	–
water–oil–gas	–	10.3
water–gas–oil	–	8.4
water–oil	–	16.0
water–gas	–	65.4

Table IV shows displacement statistics for the first gas injection and secondary water flooding cycles. While direct gas–water and water–gas displacements are most common, there are a significant number of double displacements.

3.2. EGERMANN ET AL'S DATA

Egermann *et al.* (2000) conducted WAG experiments on a water-wet Estaillades limestone core sample. Although carbonate samples usually have very complex pore structures, the inferred pore size distribution for this core is fairly close to that of our Berea sandstone network (Egermann *et al.*, 2000). Experimental gas and water relative permeabilities were obtained by history matching the production curves. Our estimated contact angles and the interfacial tensions measured in the experiments are given in Table V. The system was assumed to be weakly water-wet in order to match waterflood residual oil saturation (Figure 11). Measured and tracked saturation paths as well as the predicted versus experimental gas and water relative permeabilities are given in Figures 11–13. The oil relative permeability was not measured in these experiments. The network model was unable to reproduce exactly the observed saturation path. This could be due to finite size effects in addition to having different pore structures for the Berea network and the limestone core. The predictions of gas relative permeability are good. Again we see that during water injection subsequent to gas injection, the gas relative permeability is lower due to gas trapping. This agrees with Oak's results. For the water relative permeability, we see the same hysteresis trend as in the Oak data, for the same reason. Both the gas and water relative permeabilities decrease for repeated cycles of gas and water injection: for the gas relative permeability this is due to trapping, while for water the conductance of water layers decreases.

Table V. The interfacial tension and contact angle values used in our model to predict the experiments performed by Egermann *et al.* (2000)

σ_{gw} (mN/m)	72.1
σ_{go} (mN/m)	27
σ_{ow} (mN/m)	40.3
θ^{r}_{gw} (degrees)	33–50
θ^{r}_{go} (degrees)	0
θ^{r}_{ow} (degrees)	40–60
θ^{a}_{gw} (degrees)	50–66
θ^{a}_{go} (degrees)	0
θ^{a}_{ow} (degrees)	60–80

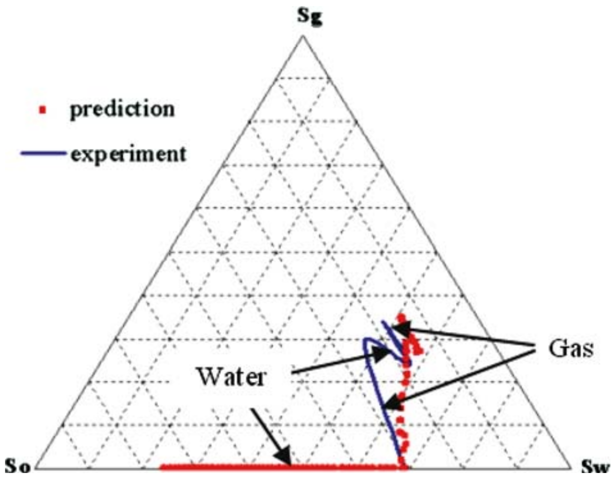

Figure 11. Comparison of measured (Egermann *et al.*, 2000) and tracked saturation paths.

3.3. ELEMENT ET AL'S DATA

Element *et al.* (2003) performed WAG experiments on water-wet Berea sandstone cores. The contact angles and spreading conditions of the experimental system were not measured. However, the high residual oil saturation after the first water injection suggests a strongly water-wet system. Estimated contact angles and interfacial tensions are given in Table VI. We assume a spreading system. Experimentally observed and tracked saturation trajectories and predicted versus measured gas relative permeabilities are shown in Figure 14 and 15, respectively. As can be seen from Figure 14, after the primary oil drainage, waterflooding is followed by gas

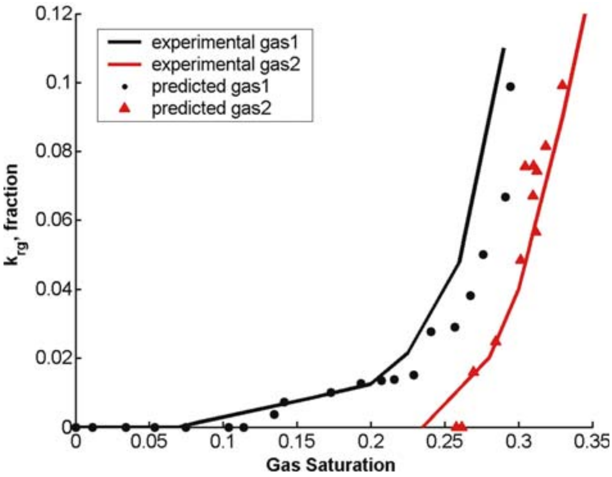

Figure 12. Comparison of measured (Egermann *et al.*, 2000) and predicted gas relative permeabilities for the saturation path shown in Figure 11.

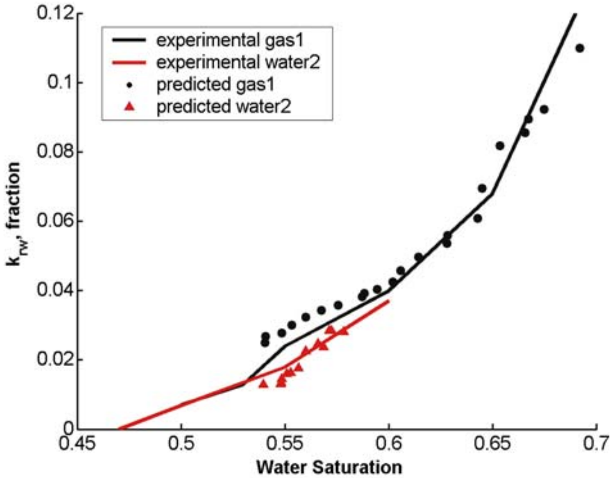

Figure 13. Comparison of measured (Egermann *et al.*, 2000) and predicted water relative permeabilities for the saturation path shown in Figure 11.

injection, water re-injection and one more gas flood. Only the gas relative permeability was measured.

We observe late gas breakthrough for our predictions due to the finite size of our network (Figure 15). However, the overall prediction of gas relative permeability is good. Again we see that the gas relative permeability is lower for the second cycle than for the first due to the trapping of gas. This again confirms the hysteresis trends observed and predicted for the previous two experiments. During both the first and second water injection

Table VI. The interfacial tension and contact angle values used in our model to predict the experiments performed by Element *et al.* (2003)

σ_{gw} (mN/m)	67
σ_{go} (mN/m)	19
σ_{ow} (mN/m)	48
θ^{r}_{gw} (degrees)	4.4–16.9
θ^{r}_{go} (degrees)	0
θ^{r}_{ow} (degrees)	0–20
θ^{a}_{gw} (degrees)	16.9–33.7
θ^{a}_{go} (degrees)	0
θ^{a}_{ow} (degrees)	20–40

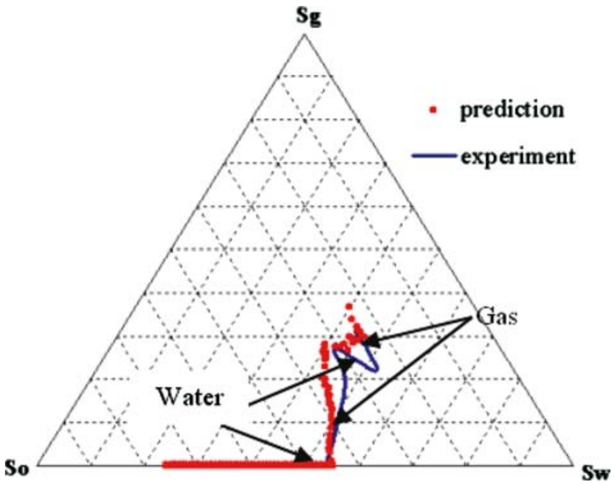

Figure 14. Comparison of measured (Element *et al.*, 2003) and tracked saturation paths.

processes we obtain more snap-off displacements (Table VII), which trap both oil and gas phases. This also results in more double displacement during subsequent gas/water injection cycles (Table VIII).

3.4. EFFECTS OF WETTABILITY

After validating our model with the available experimental data, we performed several generic WAG studies for different wettability conditions and saturation paths. We first conduct a simulation for a water-wet system. We use same contact angles and interfacial tensions that we used while predicting Oak's experiments (Oak, 1990) (Table II). The saturation path is shown in Figure 16 and the predicted gas relative permeabilities are shown

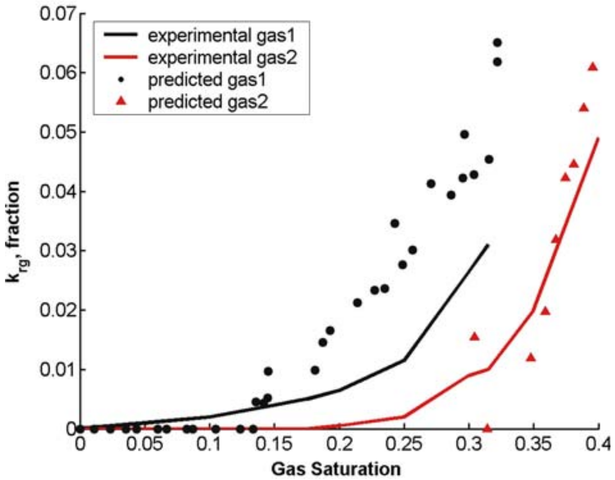

Figure 15. Comparison of measured (Element *et al.*, 2003) and predicted gas relative permeabilities for the saturation path shown in Figure 14.

Table VII. Displacement statistics of the first and second water injection cycles for the saturation path shown in Figure 14

	Piston-like (water–oil)	Snap-off (water–oil)	Layer collapse (water–oil)	Piston-like (water–gas)	Snap-off (water–gas)
1st cycle	20,858	5874	–	–	–
1st cycle (%)	78	22	–	–	–
2nd cycle	1375	47	4557	4227	616
2nd cycle (%)	12.7	0.43	42.1	39.1	5.7

Table VIII. Displacement statistics of subsequent injection cycles for the saturation path shown in Figure 14

Type/Cycle	1st gas cyle (%)	2nd water cycle (%)	2nd gas cycle (%)
gas–oil–water	8.8	–	49.2
gas–oil	74.8	–	3.2
gas–water	16.4	–	47.6
water–oil–gas	–	12.8	–
water–gas–oil	–	14.1	–
water–oil	–	38.3	–
water–gas	–	34.9	–

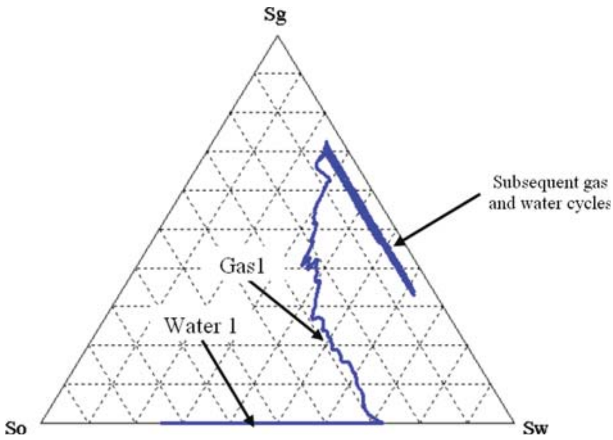

Figure 16. WAG saturation path for a water-wet system.

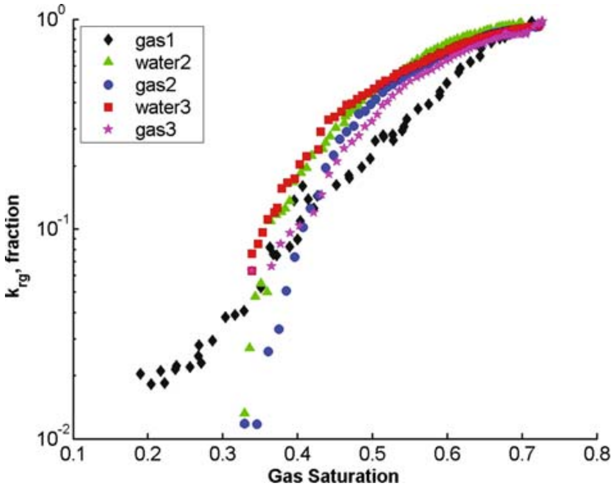

Figure 17. Predicted gas relative permeabilities for the saturation path shown in Figure 16.

in Figure 17. We do not show the water and oil relative permeabilities since they are similar to those presented for the prediction of the Oak data (Figures 7 and 8). We inject water after primary oil drainage until we reach a residual oil saturation of 28%. Then we perform a gas cycle until the oil saturation drops to about 7%. We continue with two more subsequent water and gas cycles. As expected, we reach very low residual oil saturation, around 3%, since the system is spreading and oil remains connected in layers.

An increase in the gas relative permeability at high gas saturations is observed after the first gas injection (Figure 16). This is because pore filling by water is favored in so-called dead-end pores that have only one connected throat that is water filled (Lenormand *et al.*, 1983). During the first gas injection, gas invades the pore space by an invasion percolation process, where pore filling is favored over piston-like advance in (smaller) throats (Wilkinson and Willemsen, 1983). At the end of gas injection the gas occupies a single connected cluster with many dead-end pores. These dead-end pores may contain a large volume, but do not contribute to the gas relative permeability. Hence filling these pores will change the saturation without altering the gas relative permeability making the waterflood gas relative permeability higher than for first gas invasion at high gas saturation (Figure 17). This effect has been discussed in the context of oil/water flow by Blunt (1997). The increase in gas relative permeability is only observed if gas is initially injected to very high saturation – in the experiments we predicted previously the maximum gas saturation reached initially was lower and this effect was not seen. This pore-filling process competes with snap-off that, as discussed before, causes disconnection of gas and a rapid drop in relative permeability – this effect dominates at lower gas saturation. There is only a slight decrease in relative permeability after repeated cycles of injection due to continued trapping of gas. However, Skauge and Larsen (1994) suggest that the gas relative permeability continues to decrease significantly with repeated flooding cycles. In our simulations gas reaches very high saturation values and displaces most of the oil in the system during the first cycle. During the subsequent water and gas injection cycles, we obtain almost identical saturation paths (Figure 16) and displacement processes. As can be seen from Tables IX and X, the displacement statistics are very similar for subsequent water and gas injection cycles with little continued trapping of oil and gas.

We now simulate WAG for an oil-wet system. The contact angles and interfacial tensions are given in Table XI. Valvatne and Blunt (2004) used similar oil–water contact angles to predict two-phase relative permeabilities. Note that the gas/water contact angles are greater than 90°, indicating that

Table IX. Displacement statistics of the secondary and tertiary water injection cycles for the saturation path shown in Figure 16

	Piston-like (water–oil)	Snap-off (water–oil)	Layer collapse (water–oil)	Piston-like (water–gas)	Snap-off (water–gas)
Water 2	62	83	1876	23674	2673
Fraction (%)	0.22	0.29	6.6	83.4	9.4
Water 3	33	45	137	23472	3658
Fraction (%)	0.12	0.16	0.50	85.8	13.3

Table X. Displacement statistics of the secondary and tertiary gas injection cycles for the saturation path shown in Figure 16

	Piston-like (gas–oil)	Layer collapse (gas–oil)	Piston-like (gas–water)
Gas 2	65	1436	27093
Fraction (%)	0.22	5.0	94.7
Gas 3	1093	1065	27293
Fraction (%)	3.7	3.6	92.7

Table XI. Interfacial tensions and contact angles used for WAG cycles into a strongly oil-wet system

σ_{gw} (mN/m)	67
σ_{go} (mN/m)	19
σ_{ow} (mN/m)	48
θ^{r}_{gw} (degrees)	100–124
θ^{r}_{go} (degrees)	45–65
θ^{r}_{ow} (degrees)	120–160
θ^{a}_{gw} (degrees)	116–136
θ^{a}_{go} (degrees)	65–85
θ^{a}_{ow} (degrees)	140–180

water is now the most non-wetting phase and gas is intermediate wet. The saturation path – gas injection after waterflooding followed by a subsequent cycle of water and then gas injection – is shown in Figure 18. Predicted oil, gas and water relative permeabilities are shown in Figures 19–21. In an oil-wet medium, oil layers are very stable and do not easily collapse, which enables very low residual oil saturations to be reached, as is evident in Figure 19. Oil is the most wetting phase and there is negligible hysteresis in the oil relative permeability. Unlike a water-wet medium, double displacement does not lead to a dramatic change in gas/oil or oil/water capillary pressure. We have fewer double displacements in an oil-wet system since there is very little trapped oil. Oil layers are stable and only collapse at low saturation values during the secondary water injection process (Table XII).

Although gas trapping is not as significant as in water-wet media, we do see a large decrease in gas relative permeability during the second injection cycle. During the first gas injection cycle, gas displaces principally oil as a non-wetting phase and occupies the larger pores and throats. For subsequent gas injection, gas principally displaces water as a wetting

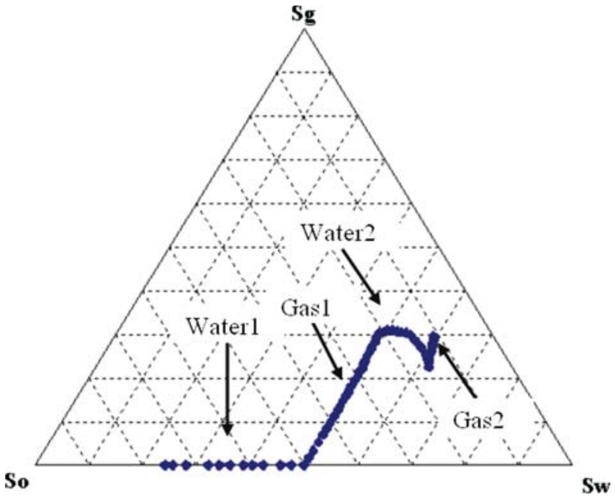

Figure 18. WAG saturation path for a strongly oil-wet system.

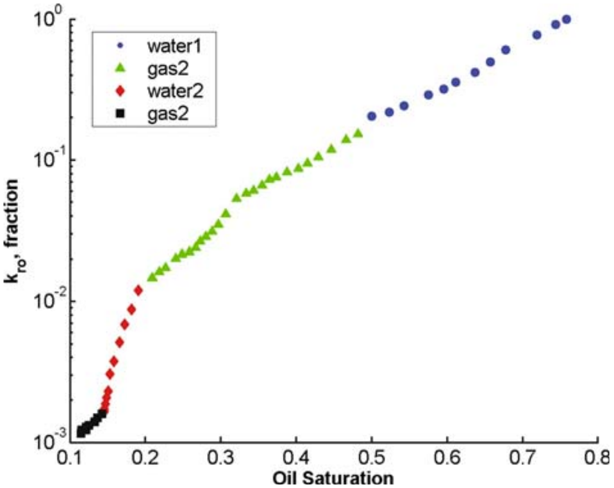

Figure 19. Predicted oil relative permeability for a strongly oil-wet system for the saturation path shown in Figure 18.

phase and occupies smaller elements – see Figure 22. As a consequence the relative permeability is substantially lower. This decrease in gas relative permeability for gas invading water in an oil-wet medium has been observed experimentally (DiCarlo *et al*., 2000a, b).

A surprising observation is that the water relative permeability – Figure 21 – is very low, except at high saturation, even though water is the most non-wetting phase. This has already been discussed in the context of two-phase flow by Valvatne and Blunt (2004). Water is connected in the corners of the pore space, but these water layers have a very low conductance giving

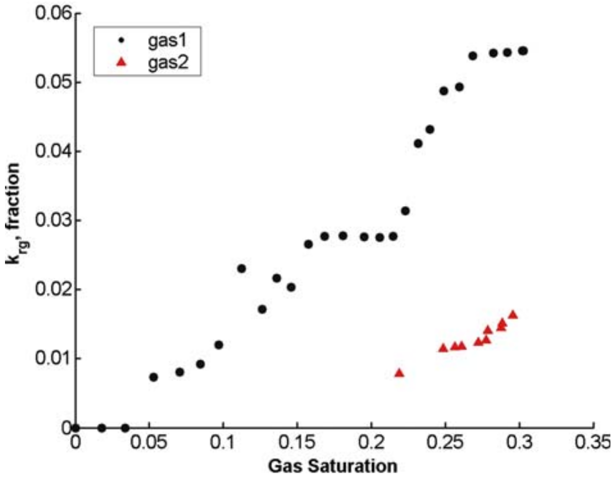

Figure 20. Predicted gas relative permeabilities for a strongly oil-wet system for the saturation path shown in Figure 18.

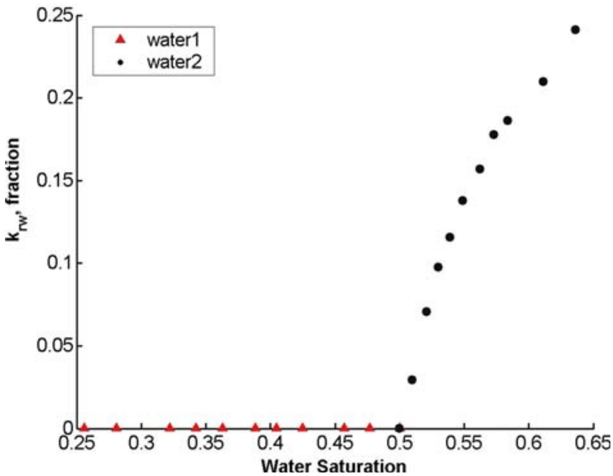

Figure 21. Predicted water relative permeabilities for a strongly oil-wet system for the saturation path shown in Figure 18.

relative permeabilities of order 10^{-6}. During water injection, water fills the larger pores and throats in clusters seeded from elements that remain water filled after primary drainage. Until these clusters connect, the water relative permeability remains very low. Only at intermediate saturation – around 0.5 – do the water clusters connect and the relative permeability increases rapidly.

Table XII. Displacement statistics of the first and second water injection cycles for the saturation path shown in Figure 18

	Piston-like (water–oil)	Snap-off (water–oil)	Layer collapse (water–oil)	Piston-like (water–gas)	Snap-off (water–gas)
Water 1	6314	0	24	–	–
Fraction (%)	99.7	0	0.3	–	–
Water 2	2923	0	12763	2594	6
Fraction (%)	16.0	0	69.8	14.2	0.03

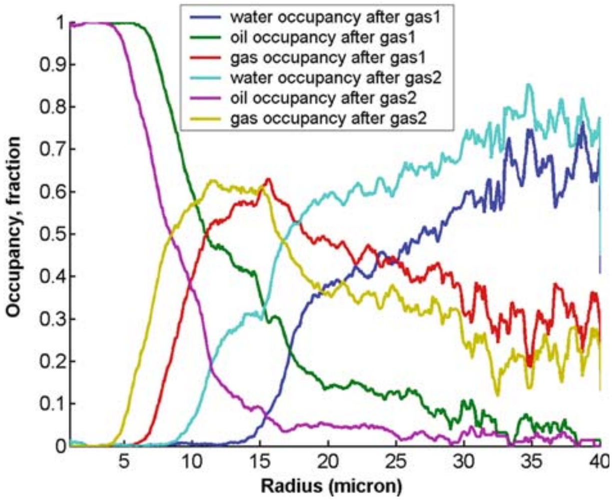

Figure 22. Pore occupancies for first and second gas injection cycles in a strongly oil-wet medium for the saturation path shown in Figure 18.

4. Discussion and Conclusions

We used a physically-based three-phase network model (Piri and Blunt, 2005a, b) to predict three-phase relative permeabilities for WAG flooding for different wettability conditions. We extended the model by adding two additional double displacement mechanisms, double imbibition (water–oil–gas) and imbibition-drainage (water–gas–oil). We first validated the model by accurately predicting relative permeabilities from three water-wet experimental datasets in the literature. We then performed a generic study of WAG flooding in water-wet and oil-wet media.

In water-wet media the gas relative permeability is lower during water injection than first gas injection because of trapping. Subsequent cycles of water and gas flooding only lead to further reductions in relative permeability if the new flooding cycles reach higher gas saturations, allowing more gas to be trapped. At high gas saturation, an increase in relative permeability after the first gas injection is predicted due to cooperative pore filling. In an oil-wet system the gas relative permeability is lower for gas invasion into water than into oil, since gas is no longer the most non-wetting phase in the presence of water.

The water relative permeability in water-wet media is lower during waterflooding when gas is present. This surprising hysteresis trend is supported by experiment. Gas injection forces trapped oil into smaller pores and throats by double displacement. When this oil reconnects during water injection, there is an increase in the oil/water capillary pressure, meaning that water layers in the corners of the pore space are thinner and have a lower conductance, resulting in a lower water relative permeability. In oil-wet media, the water relative permeability remains very low until connected clusters of water-filled elements span the system, at which point the relative permeability rises rapidly.

The oil relative permeability in water-wet media increases rapidly when gas is injected into waterflood residual oil, since oil becomes reconnected due to double drainage. The residual oil saturation can be very low if oil remains connected in spreading layers. In oil-wet media, the oil relative permeability increases monotonically with oil saturation with little hysteresis, since oil is the most wetting phase and always occupies the smaller elements or resides in stable layers. The residual saturation is very low due to the connectivity of wetting layers.

To capture these complex hysteresis trends requires a model that captures the subtleties of layer flow and different displacement processes. Current empirical relative permeability models are unable to capture this behavior (Element, 2003; Spiteri and Juanes, 2004). Pore-scale network modeling, validated through predictions of available data, could be used to develop more accurate and physically-based predictive models of three-phase relative permeability (Blunt, 2000).

Acknowledgements

We would like to thank the sponsors of the Imperial College Consortium on Pore-Scale Modelling (BHP, JOGMEC, Saudi Aramco, Schlumberger, Shell, Statoil and Total) for financial support.

References

Baker, L. E.: 1988, Three-Phase Relative Permeability Correlations, SPE 17369, in: *Proceedings of SPE/DOE EOR Symposium*, Tulsa, OK.

Blunt, M., King, P. and Scher, H.: 1992, Simulation and theory of two-phase flow in porous media, *Phys. Rev. A* **46**(12), 7680–7699.

Blunt, M. J.: 1997, Pore level modeling of the effects of wettability, *SPEJ* **2**(4), 494–510.

Blunt, M. J.: 2000, An empirical model for three-phase relative permeability, *SPEJ* **5**(4), 435–445.

Caudle, B. H. and Dyes, A. B.: 1958, Improving miscible displacement by gas–water injection, *Trans. Am. Inst. Mining Metall. Petroleum Eng.* **213**, 281–284.

Christensen, J. R., Stenby, E. H., and Skauge, A.: 1998, Review of WAG Field Experience, SPE 39883, in: *Proceedings of SPE International Petroleum Conference and Exhibition*, Villahermose, Mexico.

DiCarlo, D. A., Sahni, A. and Blunt, M. J.: 2000a, Three-phase relative permeability of water-wet, oil-wet, and mixed-wet sandpacks, *SPEJ* **5**(1), 82–91.

DiCarlo, D. A., Sahni, A. and Blunt, M. J.: 2000b, The effect of wettability on three-phase relative permeability, *Transport Porous Med.* **39**(3), 347–366.

Egermann, P., Vizika, O., Dallet, L., Requin, C. and Sonier, F.: 2000, Hysteresis in three-phase flow: Experiments, Modelling and Reservoir Simulations, in: *Proceedings of the IEA Workshop and Symposium on EOR*, Edinburgh.

Element, D. J., Masters, J. H. K., Sargent, N. C., Jayasekera, A. J. and Goodyear, S. G.: 2003, Assessment of three-phase relative permeability models using Laboratory Hysteresis Data, SPE 84903, in: *Proceedings of the SPE International Improved Oil Recovery Conference in Asia Pacific*, Kuala Lumpur, Malaysia.

Feng, Q., Di, L., Tang, G., Chen, Z., Wang, X. and Zou, J.: 2004, A Visual Micro-Model Study: The Mechanism of Water Alternative Gas Displacement in Porous Media, SPE 89362, in: *Proceedings of SPE/DOE Symposium on Improved Oil Recovery*, Tulsa, Oklahoma.

Fenwick, D. H. and Blunt, M. J.: 1998a, Network modeling of three-phase flow in porous media, *SPEJ* **3**(1), 86–97.

Fenwick, D. H. and Blunt, M. J.: 1998b, Three-dimensional modeling of three-phase imbibition and drainage, *Adv. Water Res.* **21**(2), 121–143.

Hui, M. H. and Blunt, M. J.: 2000, Effects of wettability on three-phase flow in porous media, *J. Phys. Chem. B* **104**(16), 3833–3845.

Keller, A. A., Blunt, M. J. and Roberts, P. V.: 1997, Micromodel observation of the role of oil layers in three-phase flow, *Transport Porous Med.* **26**(3), 277–297

Lake, L. W.: 1989, *Enhanced Oil Recovery*, Prentice-Hall, Englewood Cliffs, NJ.

Land, C. S.: 1968, Calculation of imbibition relative permeability for two- and three-phase flow from rock properties, *SPEJ*, 149–156.

Lenormand, R., Zarcone C. and Sarr A.: 1983, Mechanisms of the displacement of one fluid by another in a network of capillary ducts, *J. Fluid Mech.* **135**, 337–353.

Mani, V. and Mohanty, K. K.: 1998, Pore-level network modeling of three-phase capillary pressure and relative permeability curves, *SPEJ* **3**, 238–248.

Oak, M. J.: 1990, Three-Phase Relative Permeability of Water-Wet Berea, SPE 20183, in: *Proceedings of the SPE/DOE Enhanced Oil Recovery Symposium*, Tulsa, Oklahoma.

Oak, M. J.: 1991, Three-Phase Relative Permeability of Intermediate-Wet Berea Sandstone, SPE 22599, in: *Proceedings of the SPE Annual Technical Conference and Exhibition*, Dallas, Texas.

Piri, M. and Blunt, M.J.: 2005a, Three-dimensional mixed-wet random pore-scale network model of two- and three-phase flow in porous media. I. model description, *Phys. Rev.* **71**(2), 026301.

Piri, M. and Blunt, M. J.: 2005b, Three-dimensional mixed-wet random pore-scale network model of two- and three-phase flow in porous media. II. Results, *Phys. Rev.* **71**(2), 026302.

Øren, P. E., Billiotte, J. and Pinczewski, W. V.: 1992, Mobilization of waterflood residual oil by gas injection for water-wet conditions, *SPEFE* **7,** 70–78.

Øren, P. E., Billiotte, J. and Pinczewski, W. V.: 1994, Pore-scale network modelling of waterflood residual oil recovery by immiscible gas flooding, SPE 27814, in: *Proceedings of the SPE/DOE Symposium on Improved Oil Recovery*, Tulsa, Oklahoma.

Øren, P. E., Bakke, S. and Arntzen, O. J.: 1998, Extending predictive capabilities to network models, *SPEJ* **3**(4), 324–326.

Øren, P. E. and Bakke, S.: 2002, Process based reconstruction of sandstones and prediction of transport properties, *Transport Porous Med.* **46**(2–3), 311–343.

Skauge, A. and Larsen, J. A.: 1994, Three-phase relative permeabilities and trapped gas measurements related to WAG processes, SCA 9421, in: *Proceedings of the International Symposium of the Society of Core Analysts*, Stavanger, Norway.

Sohrabi, M., Henderson, G. D., Tehrani, D. H. and Danesh, A.: 2000, Visualisation of oil recovery by water alternating gas (WAG) injection using high pressure micromodels water-wet system, SPE 63000, in: *Proceedings of SPE ATCE*, Dallas, Texas.

Spiteri, E. J. and Juanes, R.: 2004, Impact of Relative Permeability Hysteresis on the Numerical Simulation of WAG Injection, SPE 89921, in: *Proceedings of SPE ATCE* Houston, Texas.

Stone, H. L.: 1970, Probability model for estimating three-phase relative permeability, *JPT* **22**(2), 214–218.

Stone, H. L.: 1973, Estimation of three-phase relative permeability and residual oil data, *JCPT* **12**(4), 53–61.

Svirsky, D. S., van Dijke, M. I. J. and Sorbie, K. S.: 2004, Prediction of three-phase relative permeabilities using a pore-scale network model anchored to two-phase data, SPE 89992, in: *Proceedings of SPE ATCE*, Houston, TX.

Valvatne, P. H. and Blunt, M. J.: 2004, Predictive pore-scale modeling of two-phase flow in mixed-wet media", *Water Resour. Res.* **40**(7), W07406.

van Dijke, M. I. J. and Sorbie, K. S.: 2002, Pore-scale network model for three-phase flow in mixed-wet porous media, *Phys. Rev. E* **66**(4), 046302.

van Dijke, M. I. J. and Sorbie, K. S.: 2003, Pore-scale modelling of three-phase flow in mixed-wet porous media: Multiple displacement chains, *J. Petrol. Sci. Eng.* **39**, 201–216.

van Dijke, M. I. J., Sorbie, K. S., Sohrabi, M., Tehrani, D. and Danesh, A.: 2004, Three-phase flow in WAG processes in mixed-wet porous media: Pore-scale network simulations and comparison with micromodel experiments, *SPEJ* **9**(1), 57–66.

van Dijke, M. I. J., Lago, M., Sorbie, K. S. and Araujo, M.: 2004, Free energy balance for three fluid phases in a capillary of arbitrarily shaped cross-section: Capillary entry pressures and layers of the intermediate-wetting phase, *J. Colloid Interface Sci.* **277**(1), 184–201.

Wilkinson, D. and Willemsen, J. F.: 1983, Invasion percolation: A new form of percolation theory, *J. Phy. A: Math. Gen.* **16**(14), 3365–3376.